Silica–poly(dimethylsiloxane) mixtures: n.m.r. approach to the crystallization of adsorbed chains

R. H. Ebengou and J. P. Cohen-Addad*
Laboratoire de Spectrométrie Physique Associé au CNRS, Université Joseph Fourier – Grenoble I, BP 87, 38402 St Martin d'Hères, France
(Received 14 June 1993; revised 9 December 1993)

This work deals with the crystallization of polymer chains within silica–poly(dimethylsiloxane) mixtures, irrespective of the type of crystalline structure that is actually present in the system. An analysis of the transverse magnetization relaxation function is proposed as a method for melting point determination as well as for determination of the extent of crystallization as a function of time during an isothermal crystallization. We first pay attention to pure poly(dimethylsiloxane) (PDMS), for which we have measured the enthalpy of fusion per mole of structural units and defined the isothermal crystallization kinetics. The results obtained for the mixtures are compared to those obtained for pure PDMS. It turns out that the presence of silica particles does not affect the dimensionality of the crystalline growth. However, it reduces the extent of crystallization and has two antagonistic effects on the overall rate of crystallization. The first is a nucleation effect which is dominant at low silica volume fractions, and the second effect is a topological constraint which becomes dominant and hinders the crystalline growth at high silica volume fractions. As a result of the competition between these two effects, the overall rate of crystallization goes through a maximum with increasing silica volume fraction.

(Keywords: silica; poly(dimethylsiloxane); n.m.r.)

INTRODUCTION

It is of both fundamental and practical interest to describe the crystallization of a polymer when it is adsorbed onto a mineral surface. For this purpose, silica–poly(dimethylsiloxane) mixtures are appropriate systems. Both the kinetics and the statistics of chain adsorption that occur in these systems have been described elsewhere[1–4]. When dealing with the crystallization of poly(dimethylsiloxane) (PDMS) chains within these systems, one may focus on two major issues. The first issue is the effect of the firm fixation of a certain number of monomeric units on the extent of crystallization. Since the overall rate of crystallization is governed by processes likely to be modified by chain adsorption, such as germination and short distance diffusion of chain segments across the phase boundary, the second issue is the effect of the topological constraints exerted on one chain, because of this adsorption, on the rate of crystallization. Additionally, recognizing the inconsistencies in the values available in the literature[5–7], it is worth defining a value for Δh_u, the enthalpy of fusion per mole of structural units for PDMS, since this parameter is important in determining the energetic aspect of the crystallization.

An X-ray diffraction study of the structure of crystalline PDMS by Damashun[8] suggested a monoclinic system with a ribbon-like, two-fold helix containing six repeat units of one chain passing through each cell. This crystalline structure, however, does not seem to be in accordance with the solid-state n.m.r. observation of the crystalline conformation of PDMS[9].

We have recently shown[10] that chain adsorption within silica–PDMS mixtures does not bring any change in either the glass transition temperature or the melting temperature of PDMS. Previous studies, which particularly dealt with the degree of crystallinity, showed that the extent of crystallization is reduced by the presence of silica particles[11,12]. However, the effect of the presence of mineral particles on the isothermal kinetics of PDMS crystallization is known in less detail.

The main goal of this work is to describe the overall kinetics of polymer crystallization within silica–PDMS mixtures, irrespective of the crystalline structure present in the mixture. An analysis of the transverse magnetization relaxation function of PDMS protons is proposed as a method for the determination of the amount of crystalline phase as a function of time.

EXPERIMENTAL

Samples

Silica–poly(dimethylsiloxane) samples were kindly supplied by Rhône–Poulenc. The surface area of the fumed silica (Aerosil 150) determined by BET methods was $150\,m^2\,g^{-1}$. A two-roll stainless steel mill was used to incorporate silica particles into the polymer. The average duration of the milling was 15 min. The number average molecular weights of the PDMS

* To whom correspondence should be addressed

0032-3861/94/14/2962–08
© 1994 Butterworth-Heinemann Ltd

chains were $\bar{M}_n = 1.8 \times 10^3$, 5.6×10^3, 42×10^3, 54×10^3, 85×10^3, 110×10^3 and 260×10^3 g mol^{-1}. The index of polydispersity was 1.9. Two values of the initial concentration of silica in the mixtures were considered, namely $c_{Si}^i = 0.17$ (w/w) and $c_{Si}^i = 0.29$ (w/w). The corresponding initial silica volume fractions were respectively $\phi_{Si}^i = 0.08$ and $\phi_{Si}^i = 0.15$. All the non-adsorbed chains were removed from the mixtures after the completion of the adsorption process to allow a study of the adsorbed layer only.

Extraction of non-adsorbed chains

The non-adsorbed polymer chains were removed from the mixtures by suspending each sample in a large excess of methylcyclohexane for two days. The solvent was renewed twice during this time interval. The residue was vacuum dried at room temperature for two days and subsequently at 90°C for another two days. The specific amount of polymer left bound to the silica surface was determined by microanalysis of the silicon–carbon ratio, and subsequently the residual silica volume fraction ϕ_{Si}^r was calculated.

N.m.r. measurements

The n.m.r. measurements were performed using a Bruker pulsed n.m.r. spectrometer operating at 60 MHz. Transverse magnetic relaxation functions of protons were obtained from spin echoes which were formed by applying Carr–Purcell sequences to the spin system. A cold nitrogen flow was used to regulate the n.m.r. probe temperature. The samples were conditioned in n.m.r. tubes sealed under vacuum. For melting point measurements, after an initial cold crystallization, the samples were heated in 2 K steps spaced out by 5 min. At the end of each 5 min period the relaxation function was recorded. For observing the crystallization kinetics, immediately after the immersion of the sample in the probe the transverse magnetization relaxation function was recorded at regular time intervals depending on the rate of the process.

USUAL DESCRIPTION OF THE OVERALL KINETICS OF POLYMERIC CRYSTALLIZATION

The usual description of the overall kinetics of polymeric crystallization uses the Avrami equation[13–15]. This equation, which relates the amount τ_c of transformed material to the time θ during which the system has undergone supercooling, is stated as follows

$$\tau_c(\theta) = \tau_c(\infty)[1 - \exp(-K\theta^n)] \quad (1)$$

Here $\tau_c(\infty)$ denotes the maximum amount of crystallinity reached after the completion of the primary crystallization process, since the Avrami treatment does not consider any secondary crystallization phenomena that can occur within the crystallized domains after their impingement. The exponent n of the Avrami equation is somehow related to the dimensionality of the crystalline growth. The factor K is temperature dependent.

We will consider the particular case of a heterogeneous nucleation, which is thought to be the most probable type of nucleation that can occur in macromolecular systems since these systems are typically heterogeneous[13–15,16–19]. For the sake of simplicity, we will consider a steady concentration N of germ nuclei per unit volume simultaneously activated. In this case, n is directly the dimensionality of the crystalline growth, and the following expressions result from the Lauritzen and Hoffman[20] theory of crystallization rate in polymers, including chain folding

$$K = K_0 N \exp\left(-\frac{n\Delta G_\eta}{k_B T}\right) \exp\left(-\frac{nK_g}{T\Delta T}\right) \quad (2a)$$

and

$$K_g(\text{regime I}) = \frac{4b_0\gamma\gamma_e T_m^0}{k_B \Delta h_f} = 2K_g(\text{regime II}) \quad (2b)$$

where k_B is the Boltzmann constant, T is the isothermal crystallization temperature and ΔT is the degree of supercooling, which is defined as the difference between the equilibrium melting temperature T_m^0 and the isothermal crystallization temperature T ($\Delta T = T_m^0 - T$). K_0 takes into account the geometric parameters of both the polymer chain and the crystalline lamella. Its temperature dependence is usually considered as less important than the temperature dependence of the exponential terms. ΔG_η denotes the free enthalpy of activation that governs the short distance diffusion of crystallizing elements across the phase boundary. Its temperature dependence is expected to be similar to the temperature dependence of the viscosity (i.e. a free volume law). At low supercooling $\Delta G_\eta / k_B T$ can be considered as temperature independent, and the main temperature dependence of the thermal factor K arises from the term $\exp(-nK_g/T\Delta T)$. $\Delta G_\eta / k_B T$ becomes infinite in the vicinity of the glass transition. The term b_0 is the b parameter of the unit cell, γ is the interfacial free energy for the lateral surface and γ_e is the interfacial free energy for the folding surface. T_m^0 is the equilibrium melting temperature. The term Δh_f is the enthalpy of fusion per unit volume of structural unit.

PRINCIPLE OF THE N.M.R OBSERVATION

Relaxation function for a semicrystalline sample

The n.m.r. approach is based on the well-known difference in the relaxation properties between protons belonging to a rigid phase, such as a crystalline phase, and those belonging to a mobile amorphous phase[21]. Consequently, the whole relaxation function recorded at time θ of the isothermal crystallization process, i.e. $M_x(t, \theta)$, consists of two components, and it can be written as

$$M_x(t, \theta) = M_{xc}(t, \theta) + M_{xa}(t, \theta) \quad (3)$$

where $M_{xc}(t, \theta)$ is the fast decay component observable at short times (10–20 μs) and ascribed to protons which belong to the crystalline phase, while $M_{xa}(t, \theta)$ is the slow decay component observable at long times and ascribed to the protons of the mobile amorphous phase. Therefore, the whole relaxation time-scale denoted by t is of the order of a few milliseconds. The θ time-scale describes the isothermal crystallization, and can be anywhere between a few minutes to a few hours. Consequently, the measurement of the relaxation function can be considered as instantaneous compared to the whole time-scale of the isothermal crystallization.

The melting point

After the completion of an isothermal crystallization the relaxation function exhibits a two-component

behaviour, as discussed earlier. As the temperature increases, the material transfer from the crystalline phase to the amorphous phase caused by the melting of metastable crystallites is associated with an increase in the weight of $M_{xa}(t, \theta)$ in the whole relaxation function. At the melting temperature the crystalline component of $M_x(t)$ vanishes. The behaviour of $M_x(t)$ with temperature is not governed by a material transfer from one phase to the other at this point, it is simply governed by the Curie law[21]. To characterize the melting, we plotted the amplitude of the magnetization at a chosen time in the slow decay time-scale *versus* temperature. As shown in *Figure 1*, this amplitude goes through a maximum as the temperature increases. The ascending part of the curve corresponds to the progressive melting of metastable crystallites, while the descending part gives evidence for non-crystalline behaviour. The maximum of the curve defines the n.m.r. melting temperature.

The amount of crystallinity

If one considers equation (3), then the amount of crystalline material at time θ can be determined from the weights of the two components in the total magnetization at any time. However, such a determination would require the exact mathematical expressions of the crystalline and amorphous components of the relaxation function, which are often not available. Nevertheless, owing to the difference between the relaxation rates of the two components of the relaxation function, it is possible to overcome this difficulty. The expression for $\tau_c(\theta)$, the amount of crystallinity at time θ of the isothermal crystallization, is stated as follows[10]

$$\tau_c(\theta)=\frac{M_x(t_0, 0)-M_x(t_0, \theta)}{M_x(0, 0)} \quad (4)$$

where $t_0=20\,\mu s$ was chosen as a convenient value for the determination of the amount of crystallinity. Equation (4) gives a maximum amount of crystallinity of approximately 40% for the pure PDMS sample.

Crystallization isotherms

Figure 2 shows typical crystallization isotherms for pure PDMS. The experimental curves are in accordance with the Avrami law as given by equation (1). The final amount of crystallinity $\tau_c(\infty)$, the exponent n and the thermal factor K were taken as fitting parameters. The isotherms were characterized by the typical time $t_{1/2}$ defined as the crystallization half-time, which is the time required for the system to achieve half of the total extent of crystallization $\tau_c(\infty)$. The term $t_{1/2}$ is related to the thermal factor K and the exponent of the Avrami equation by the expression

$$t_{1/2}=\left(\frac{\ln 2}{K}\right)^{1/n} \quad (5)$$

We also defined the crystallization rate as the inverse of the typical time $t_{1/2}$.

Crystallization kinetics observed from the amorphous phase

It is now well established that the nuclear magnetization observed from a polymeric system can reflect the existence of topological constraints on a semilocal space scale[22]. Such constraints are responsible for residual tensorial interactions that govern the transverse magnetization relaxation. This property allows one to follow the development of a crystalline phase from the relaxational response of protons linked to segments belonging to the mobile amorphous phase.

From the amorphous phase standpoint, the appearance of crystallites can be thought of as the development of new topological constraints which generate residual tensorial interactions. Consequently, the higher the extent of crystallization, the faster is the relaxation for the amorphous component of the whole relaxation function. *Figure 3* shows the typical evolution of the relaxation

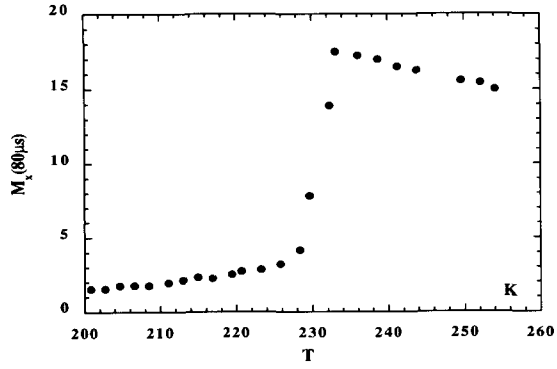

Figure 1 The amplitude M_x (80 μs) of the transverse magnetization at $t=80\,\mu s$ as a function of temperature

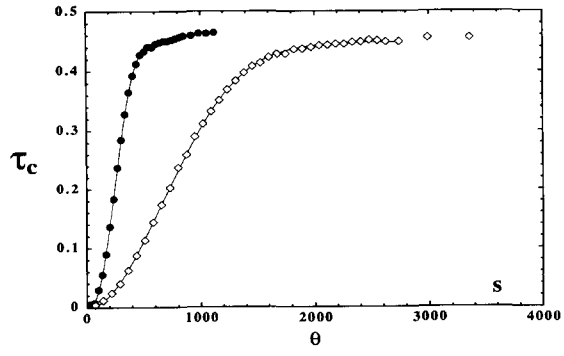

Figure 2 Crystallization isotherms observed for pure PDMS having a number average molecular weight $\bar{M}_n=54\times10^3\,g\,mol^{-1}$. The crystallization temperatures were 205 K (●) and 210 K (◇). The solid curves are plots of the Avrami equation

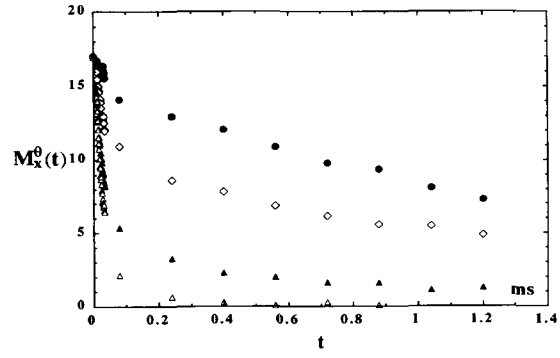

Figure 3 Typical evolution of the relaxation function during the isothermal crystallization. The different transverse magnetic relaxation curves correspond to different times (θ) during which the system has undergone supercooling: (●) $\theta=0$; (◇) $\theta=320$ s; (▲) $\theta=640$ s; (△) $\theta=1600$ s

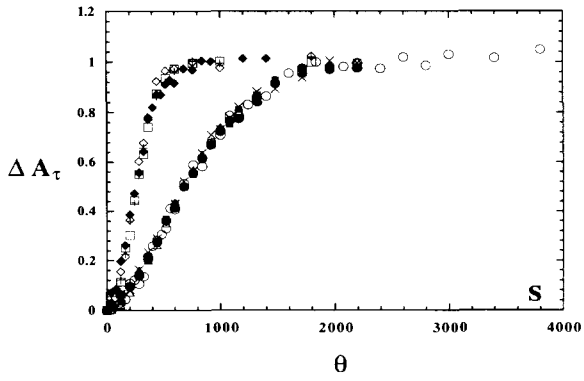

Figure 4 The variable ΔA_τ as a function of the crystallization time θ for pure PDMS having a number average molecular weight $\bar{M}_n = 260 \times 10^3$ g mol^{-1} and a corresponding silica-filled sample with a residual silica volume fraction of $\phi_{Si}^r = 0.2$. The crystallization isotherms are independent of the choice of the time τ. For pure PDMS: (○) $\tau = 0.02$ ms; (×) $\tau = 0.08$ ms; (△) $\tau = 0.4$ ms; (●) $\tau = 0.72$ ms; (■) $\tau = 1.2$ ms. For the filled sample: (◆) $\tau = 0.02$ ms; (+) $\tau = 0.24$ ms; (□) $\tau = 0.56$ ms; (◇) $\tau = 1.2$ ms

function during the isothermal crystallization. We defined the variable $\Delta A_\tau(\theta)$ as

$$\Delta A_\tau(\theta) = \frac{M_x(\tau, 0) - M_x(\tau, 0)}{M_x(\tau, 0) - M_x(\tau, \infty)} \quad (6)$$

$\Delta A_\tau(\theta)$ represents the normalized variation of the amplitude of the transverse magnetization at time τ, observed from the beginning to time θ of the isothermal crystallization ($\Delta A_\tau(0) = 0$ and $\Delta A_\tau(\infty) = 1$). As shown in *Figure 4*, the curves corresponding to different values of τ coincide, suggesting that the kinetics are independent of the choice of the time τ. Furthermore, all of the curves coincide with that describing the evolution of the normalized amount of crystallinity, $\tau_c(\theta)/\tau_c(\infty)$. In fact, it is obvious from equations (4) and (6) that $\tau_c(\theta)/\tau_c(\infty)$ is equal to $\Delta A_{20\mu s}(\theta)$.

From these results one can conclude that for a crystallizing sample, the evolution of the relaxation function of the transverse magnetization observed both from protons in the crystalline phase and from protons in the amorphous phase defines a unique isotherm. This treatment is, moreover, independent of the absolute value of the amount of crystallinity, which usually depends on the experimental technique used for the measurements.

ENTHALPY OF FUSION PER MOLE OF STRUCTURAL UNITS

N.m.r. values for T_m were measured on PDMS solutions in deuterated toluene for solvent volume fractions ranging from 0 to 0.4. The corresponding T_m values are listed in *Table 1*. These results are in good agreement with Flory's equation[23] for melting point depression by solvent addition, and the value of the enthalpy of fusion per mole of PDMS structural units obtained from the numerical fit was 5.4 ± 0.3 kJ mol^{-1}. This value is in good agreement with that (4.7 kJ mol^{-1}) given by Andrianov *et al.*[6,7] and is twice that (2.7 kJ mol^{-1}) given by Lee *et al.*[5].

RATE OF CRYSTALLIZATION IN PURE PDMS

Before considering the crystallization of PDMS chains in loaded systems, we will first describe the kinetics of crystallization in pure PDMS.

Table 1 N.m.r. melting temperatures for slightly dilute PDMS solutions in deuterated toluene

Solvent volume fraction	Melting temperature (K)
0	239 ± 2
0.1	233 ± 2
0.2	228 ± 2
0.3	225 ± 2
0.4	223 ± 2

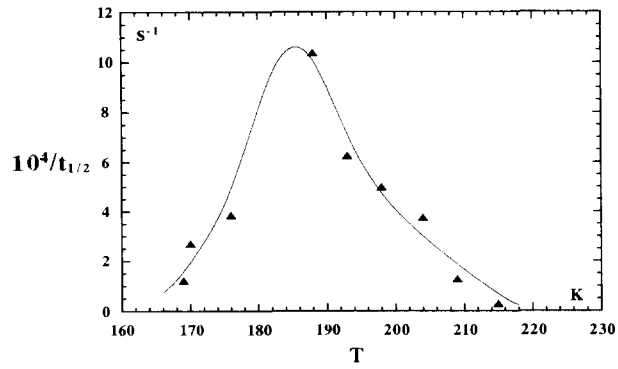

Figure 5 The overall rate of crystallization $t_{1/2}^{-1}$ as a function of temperature for pure PDMS having a number average molecular weight $\bar{M}_n = 54 \times 10^3$ g mol^{-1}

Temperature effect

We observed the isothermal crystallization of a pure PDMS sample with a number average molecular weight $\bar{M}_n = 54 \times 10^3$ g mol^{-1} within the temperature range 170–220 K.

As shown in *Figure 5*, the rate of crystallization passes through a maximum with increasing temperature. This behaviour, common in the crystallization of polymeric systems, is specific to the $\exp(-\Delta G_\eta/k_B T)\exp(-K_g/T\Delta T)$ temperature dependence of the overall rate of crystallization, as discussed earlier. Thus, the rate of crystallization approaches zero in the vicinity of the glass transition temperature since the activation energy for the transport of crystallizing elements becomes infinite, and it also approaches zero in the vicinity of the melting temperature since $\Delta T = 0$. The temperature of maximum crystallization rate for pure PDMS was found to be about 185 K.

Interfacial free energies of PDMS crystallites

It is worth emphasizing the specific behaviour of the crystallization rate in the low supercooling range, which is at temperatures above the temperature of maximum crystallization rate. In this temperature range one can reasonably consider $\Delta G_\eta/k_B T$ as temperature independent. Consequently, according to equations (2a) and (5), the logarithm of the inverse of the crystallization half-time should depend linearly on the parameter $1/T\Delta T$. *Figure 6* shows the plots of the logarithm of the crystallization rate against $1/T\Delta T$ for two PDMS samples of different molecular weights. From the slope of the straight line variation observed, the product $\gamma\gamma_e$ of the interfacial free energy of the lateral surface and the interfacial free energy of the folding surface was calculated for PDMS crystalline lamellae. Equation (2a) for K_g was used and regime I was considered, since no regime transition was observed within the whole temperature

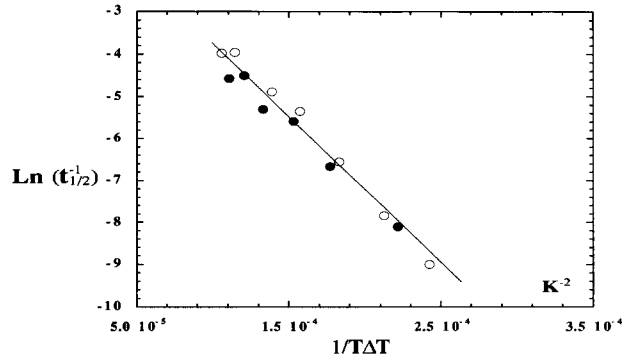

Figure 6 Logarithm of the overall rate of crystallization *versus* $1/T\Delta T$ for pure PDMS samples having number average molecular weights $\bar{M}_n = 54 \times 10^3$ g mol^{-1} (●) and $\bar{M}_n = 260 \times 10^3$ g mol^{-1} (○)

Table 2 Rates of crystallization for pure PDMS

$10^{-3}\bar{M}_n$ (g mol^{-1})	Isothermal crystallization rate $t_{1/2}^{-1}$ (s^{-1})	
	T=214 K	T=217 K
42	2×10^{-4}	
110	2.65×10^{-4}	6.11×10^{-5}
260	3.92×10^{-4}	9.64×10^{-5}

range. We used the values[5,8] $b_0 = 8.3$ Å $= 8.3 \times 10^{-8}$ cm, $T_m^0 = 236$ K, $k_B = 1.38 \times 10^{-23}$ J K^{-1} $= 1.38 \times 10^{-16}$ erg K^{-1} and $\Delta h_f = 5.4$ kJ mol^{-1} $= 7.82 \times 10^8$ erg cm^{-3}. The value of the product is $\gamma\gamma_e = 53 \pm 3$ erg^2 cm^{-4}. Estimating the value of γ, the interfacial free energy for the lateral surface, using the empirical law $\gamma = 10^{-1}\Delta h_f b_0$, one obtains $\gamma = 6.5$ erg cm^{-2} for the lateral surface interfacial free energy and $\gamma_e = 8.2$ erg cm^{-2} for the folding surface interfacial free energy.

Work of chain folding

The work q of chain folding is usually expressed as

$$q = 2a_0 b_0 \gamma_e \quad (7)$$

where a_0 and b_0 are respectively the a and b parameters of the unit cell. Using the value[5] $a_0 = 13$ Å for the PDMS unit cell, one obtains a value of $q = 17.7 \times 10^{-14}$ erg. This value, which is low compared to those available for other polymers[16], is reflective of the flexibility of the PDMS backbone, which has been reported as being particularly high[24].

Molecular weight effect

As shown in *Table 2*, the overall crystallization rate of pure PDMS increases with increasing molecular weight. This behaviour is atypical for crystallizing polymeric systems. Generally, an increase in the viscosity of a pure polymer resulting from an increase in the molecular weight induces an increase in ΔG_η, the free enthalpy barrier for the transport of crystallizing elements across the phase boundary. Thus, one usually expects the crystallization rate to be lowered when the molecular weight is increased. For PDMS, previous studies using neutron scattering[17] suggested the presence of interrupted helical conformations in the molten state. These fluctuating interrupted helices were shown to be stabilized by an increase in the viscosity or a lowering of the temperature. Moreover, it is known from analysis of high resolution n.m.r. spectra that high molecular weight PDMS does not exhibit a pure liquid-like behaviour[25]. One may conclude that, owing to their flexibility, PDMS chains have a tendency for helical conformations. These ordered chain portions can behave as germ nuclei whenever the system is undercooled, and subsequently initiate the crystallization. Since these germs are stabilized by the viscosity, the higher is the molecular weight, the faster is the crystallization rate.

RATE OF CRYSTALLIZATION IN LOADED SYSTEMS

Evidence for a silica particle induced nucleation

We observed the overall crystallization rate for two loaded samples, involving the same PDMS chains as discussed earlier, over a wide temperature range. The residual silica volume fractions after the removal of the non-adsorbed chains were $\phi_{Si}^r = 0.14$ and $\phi_{Si}^r = 0.19$.

Figure 7 shows the behaviour of the crystallization rate against temperature for these two loaded systems compared to that observed for pure PDMS. It is apparent from this figure that the maximum crystallization rate is shifted towards higher temperatures in the loaded systems. Instead of 185 K as measured for pure PDMS, the maximum is located at 200 K for the loaded samples. No difference was observed between the two loaded samples within the experimental accuracy. One interpretation of these results suggests evidence for a nucleation effect induced by the presence of silica particles in the mixtures. In agreement with previous findings[26,27], it can be assumed that the presence of a foreign surface lowers the free enthalpy barrier for the formation of critical nuclei and increases the concentration of heterogeneous nuclei at a given temperature. Consequently, a higher rate of crystallization requires less supercooling in the case when the systems are loaded.

Overall rate of crystallization: characteristic behaviour

Figure 8 shows plots of the overall crystallization rate *versus* the residual volume fraction of silica for the mixtures. These curves, which exhibit a maximum at a certain silica volume fraction, are characteristic of the crystallization of PDMS in the presence of silica particles. Such a behaviour has been found to be independent of the crystallization temperature within the low supercooling temperature range, although the

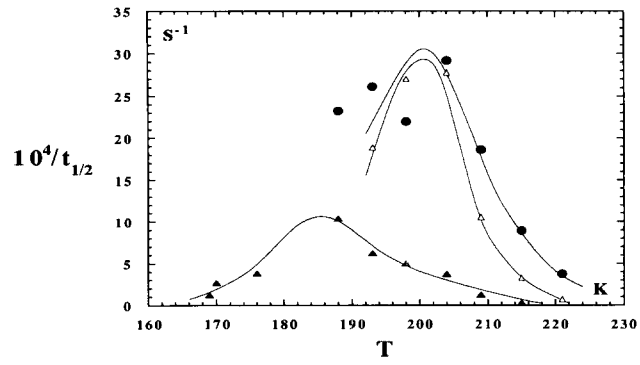

Figure 7 Overall rate of crystallization $t_{1/2}^{-1}$ as a function of temperature for pure PDMS having a number average molecular weight $\bar{M}_n = 54 \times 10^3$ g mol^{-1} (▲) and for two corresponding silica-filled samples with residual silica volume fractions $\phi_{Si}^r = 0.08$ (●) and $\phi_{Si}^r = 0.15$ (△)

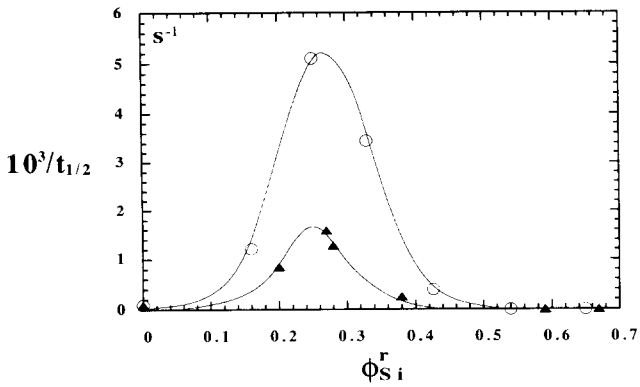

Figure 8 Overall rate of crystallization as a function of the residual silica volume fraction within the mixture for two initial silica volume fractions, $\phi^i_{Si}=0.08$ (○) and $\phi^i_{Si}=0.15$ (▲). The crystallization temperature was 217 K

absolute value of the crystallization rate is temperature dependent. This characteristic behaviour suggests that, in addition to the nucleation role discussed earlier, the silica particles may also constrain the crystalline growth by an impingement mechanism. This effect is likely to hinder the material ordering when the silica volume fraction becomes high.

Low silica volume fractions. For silica volume fractions less than $\phi^r_{Si}=0.26$, the nucleation role is dominant. At these silica volume fractions, the adsorption points are far from one another and the segmental mobility within the loops between two adsorption points is important. Therefore, the organization of the adsorbed layer, although not yet crystalline, favours ordering when the system is undercooled. In this silica volume fraction range the crystallization rate increases with increasing silica concentration.

High silica volume fractions. For silica volume fractions greater than $\phi^r_{Si}=0.26$, the silica particles essentially play the role of spatial constraints to crystalline growth. The rate of crystallization vanishes with increasing silica volume fraction. A zero crystallization rate is reached for $\phi^r_{Si}=0.45$. Above this critical silica volume fraction, according to previous studies[3,4], one can visualize that the number of adsorbed monomeric units per chain becomes such that not enough material is available between consecutive adsorbed monomers along one chain to allow the formation of PDMS crystalline conformations. For example, let us consider the sample corresponding to a residual silica volume fraction of $\phi^r_{Si}=0.65$ and an initial silica volume fraction of $\phi^i_{Si}=0.08$. The molecular weight of the corresponding PDMS chain is $\bar{M}_n=1.8\times10^3\,g\,mol^{-1}$, where about one out of five monomers is firmly fixed onto the silica surface. Since such statistics of chain fixation are not compatible with the crystalline PDMS unit cell[8], such a mixture could not develop PDMS crystalline domains.

Maximum rate of crystallization. As a result of the competition between the two effects discussed above, the crystallization rate exhibits a maximum between the extreme silica volume fractions. The corresponding silica volume fraction for a maximum rate of crystallization is about $\phi^r_{Si}=0.26$.

Influence of the initial silica concentration. The two curves in *Figure 8* show that the crystallization is faster for the lower initial silica volume fractions. These differences were attributed to the difference between the percolation states for the two initial silica concentrations. It has recently been shown[28] that the state of percolation for a silica–PDMS mixture depends both on the initial silica concentration and on the amount of polymer bound to the silica surface. Moreover, previous n.m.r. studies[4] have shown that the amount of fixed monomers is higher for high initial silica concentrations. Therefore, for high initial silica concentrations the degree of constraints per chain is higher. This lowers the mobility of the crystallizing elements and, as a consequence, lowers the overall crystalline rate.

AMOUNT OF CRYSTALLINITY AND AVRAMI EXPONENTS

Amount of crystallinity

Some values of $\tau_c(\infty)$, the amount of crystallinity after the completion of the crystallization process, are listed in *Table 3*. The amount of crystallinity is roughly a decreasing function of the residual silica volume fraction. We found that $\tau_c(\infty)$ was about 40% for pure PDMS, irrespective of the molecular weight, while it was zero for residual silica volume fractions greater than $\phi^r_{Si}=0.45$. As discussed above, this silica volume fraction dependence of the extent of crystallization is consistent with an increasing amount of fixed and subsequently uncrystallizable material with increasing silica volume fraction. The same behaviour has also been observed through differential scanning calorimetry measurements[11,12].

Avrami exponents

If we assume heterogeneous germination, which is a reasonable assumption for crystallizing PDMS in the presence of mineral particles, then the Avrami exponent n denotes the dimensionality of the growth. No difference in the growth dimensionality was observed between the pure PDMS and the loaded systems. The average Avrami exponent found was $n=2.1\pm0.2$ for both cases.

ENERGETIC ASPECTS OF THE CRYSTALLIZATION OF THE ADSORBED LAYER

In this section, we specify the temperature dependence (at low supercoolings) of the crystallization rate in silica–PDMS mixtures for different silica volume fractions.

Table 3 Amounts of crystallinity after the completion of the crystallization process and the corresponding silica volume fractions

$\phi^i_{Si}=0.08$		$\phi^i_{Si}=0.15$	
ϕ^r_{Si}	$\tau_c(\infty)$	ϕ^r_{Si}	$\tau_c(\infty)$
0.0	0.40 ± 0.03	0.0	0.40 ± 0.03
0.16	0.30 ± 0.01	0.20	0.30 ± 0.01
0.25	0.31 ± 0.01	0.27	0.30 ± 0.01
0.33	0.30 ± 0.01	0.28	0.30 ± 0.01
0.43	0.25 ± 0.008	0.38	0.24 ± 0.007
0.54	0.0	0.59	0.00
0.65	0.0	0.67	0.00

The treatment discussed earlier, which led to an estimate of the work of chain folding for PDMS, is less justifiable for loaded systems, since information on the organization of adsorbed PDMS chains within the crystalline domains is not available. However, it is still realistic to relate the kinetic properties of PDMS chain crystallization in loaded systems to an apparent free enthalpy barrier which governs the overall process of development of the new phase. From this point of view, the dependence of the interfacial energies on this barrier is not relevant information.

Free enthalpy barrier for crystallization and concentration of germ nuclei

We rewrite equation (2a) for the thermal factor K as

$$K = K_0 N \exp\left(-\frac{n\Delta G_\eta}{k_B T}\right)\exp\left(-\frac{\Delta G_a^*}{k_B T}\right) \quad (8)$$

where we defined ΔG_a^* as

$$\Delta G_a^* = \frac{k_B K_g}{\Delta T} \quad (9)$$

We define ΔG_a^* as an apparent free enthalpy barrier for crystallization which depends on the degree of supercooling. In the particular case of a heterogeneous germination, the Lauritzen and Hoffman theory[20] gives the $1/\Delta T$ dependence of equation (9). For a two-dimensional growth at low supercoolings, it can be seen from equations (5) and (8) that the logarithm of the inverse of the crystallization half-time can be expressed as

$$\ln(t_{1/2}^{-1}) = \frac{1}{2}\left[\ln N(\phi_{Si}^r) + \ln\frac{K_0}{\ln 2}\right] - \frac{\Delta G_a^*}{k_B T} \quad (10)$$

Without any loss of generality, one can assume that in the presence of silica particles, the concentration N of germ nuclei per unit volume depends on the residual silica volume fraction.

Similarly to the behaviour observed for pure PDMS (*Figure 6*) and in agreement with the $1/\Delta T$ dependence of the apparent free enthalpy barrier (equation (9)), the logarithm of the overall crystallization rate showed a linear dependence on the parameter $1/T\Delta T$. However, the slope of the straight line was silica volume fraction dependent and allowed a caluclation of ΔG_a^* for various silica volume fractions. Furthermore, at a given supercooling, both the values of $\Delta G_a^*/k_B T$ and $\ln(t_{1/2}^{-1})$ are completely experimentally determined. Consequently, according to equation (10) the variation with the silica volume fraction of the sum $\Delta G_a^*/k_B T + \ln(t_{1/2}^{-1})$ describes qualitatively the variation of the logarithm of the germ nuclei concentration per unit volume. For the sake of simplicity, we assume the first term of the right-hand side of equation (10) to be silica volume fraction independent.

For all the crystallizable loaded samples considered in this work, the corresponding experimental values are listed in *Table 4*. It is seen that while the apparent free enthalpy barrier $\Delta G_a^*(\phi_{Si}^r)$ goes through a minimum, the concentration of germ nuclei $N(\phi_{Si}^r)$ is roughly an increasing function of the silica volume fraction. These observations are consistent with both the characteristic behaviour of the overall crystallization rate *versus* silica volume fraction and a nucleation effect induced by the silica particles.

CONCLUSIONS

The kinetics of crystallization of PDMS in the presence of silica particles have been investigated. The results discussed in the present paper have concerned mainly the dependence of the overall crystallization rate on the silica volume fraction.

An initial investigation was completed in order to define the crystallization for pure PDMS, for which we have also measured the enthalpy of fusion per mole of structural units. The molecular weight dependence of the crystallization rate for pure PDMS is in contrast with the common behaviour usually observed for most polymers. The work of chain folding for PDMS evaluated from the temperature dependence of the rate of crystallization at low supercoolings is consistent with the high flexibility of the PDMS backbone already reported[23].

With regard to the silica–PDMS mixtures, it is worth noting the good agreement between the kinetic properties of PDMS chain crystallization presented in this work and the statistics of PDMS chain adsorption[3,4]. We have shown that the extent of crystallization is reduced by the presence of silica particles, while the dimensionality of the crystal growth is not affected. The overall crystallization of PDMS chains can be described as a process governed by two parameters which were found experimentally to be silica volume fraction dependent. These are the steady concentration of germ nuclei per unit volume N and the apparent free enthalpy barrier for the overal crystallization ΔG_a^*. The silica volume fraction dependence of these two parameters is in agreement with the characteristic silica volume fraction dependence of the overall rate of crystallization. While N increases monotonically with increasing silica volume fraction, ΔG_a^* goes through a minimum.

These results emphasize the double role played by silica particles in crystallizing the PDMS within silica-filled samples. At low silica volume fractions, nucleation

Table 4 Silica volume fraction dependence of the crystallization half-time, the apparent free enthalpy barrier and the primary germ concentration

	$\phi_{Si}^i = 0.08$				$\phi_{Si}^i = 0.15$		
ϕ_{Si}^r	$t_{1/2}$ (s)	$\Delta G_a^*/k_B T$	$\frac{1}{2}\left[\ln N(\phi_{Si}^r) + \ln\frac{K_0}{\ln 2}\right]$	ϕ_{Si}^r	$t_{1/2}$ (s)	$\Delta G_a^*/k_B T$	$\frac{1}{2}\left[\ln N(\phi_{Si}^r) + \ln\frac{K_0}{\ln 2}\right]$
0	5000±60	7.55±0.08	−1.00±0.10	0			
0.16	376±30	4.55±0.05	−1.38±0.15	0.20	580±30	5.70±0.06	−0.66±0.07
0.26	140±30	3.61±0.04	−1.33±0.09	0.26	210±30	6.27±0.06	0.92±0.11
0.30	143±30	4.70±0.05	−0.26±0.04	0.28	200±30	9.11±0.09	3.86±0.5
0.42	750±30	8.26±0.08	1.63±0.17	0.38	300±30	15.95±0.15	10.24±1.2

effects are dominant and adding an amount of silica to the polymer melt accelerates the crystallization kinetics. At high silica concentrations, the silica particles constrain spatially the crystalline growth. This results in the crystallization kinetics slowing down with further additions of silica. As a consequence of the latter effect, samples with very high silica volume fractions, i.e. $\phi_{Si}^{r} \geqslant 0.45$, do not show any crystallization phenomena.

REFERENCES

1 Cohen-Addad, J. P., Huchot, Ph., Jost, Ph. and Pouchelon, A. *Polymer* 1989, **30**, 143
2 Cohen-Addad, J. P. and Girard, O. *Polymer* 1991, **32**, 860
3 Cohen-Addad, J. P. *Polymer* 1989, **30**, 1820
4 Cohen-Addad, J. P. and Ebengou, R. H. *Polymer* 1992, **33**, 379
5 Lee, C. L., Johannson, O. K., Flaningam, O. L. and Hahn, P. *Polym. Prepr.* 1969, **10**, 1331
6 Andrianov, K. A., Zhdanov, A. A., Slonimsky, G. L., Levin, V. Yu. and Godovsky, K. Yu. *Vysokomol. Soedin., Ser. A* 1969, **11**, 2444
7 Andrianov, K. A., Zhdanov, A. A., Tsvankin, D. Ya., Levin, V. Yu., Moskalenko, V. A., Slonimsky, V. Yu. and Galil-Ogly, F. A. *Vysokomol. Soedin., Ser. A* 1971, **13**, 2685
8 Damashun, G. *Kolloid Z.* 1962, **180**, 65
9 Tonelli, A. E., Gomez, M. A. and Schilling, F. C. *Macromolecules* 1991, **24**, 6552
10 Ebengou, R. H. PhD thesis, Université Joseph Fourier – Grenoble I, France, 1992
11 Clarson, S. J., Marik, J. E. and Dodgson, K. *Polym. Commun.* 1988, **29**, 208
12 Bordeaux, D. and Cohen-Addad, J. P. *Polymer* 1990, **31**, 743
13 Avrami, M. *J. Chem. Phys.* 1939, **7**, 1103
14 Avrami, M. *J. Chem. Phys.* 1940, **8**, 212
15 Avrami, M. *J. Chem. Phys.* 1941, **9**, 177
16 Wunderlich, B. 'Macromolecular Physics', Vol. 2, Academic Press, New York, 1976
17 Henry, A. W. and Safford, G. J. *J. Polym. Sci. (A-2)* 1969, **7**, 433
18 Laridjani, M., Pouget, J. P., Scherr, E. M., MacDiarmid, A. G., Josefowicz, M. E. and Epstein, A. J. *Macromolecules* 1992, **25**, 4106
19 Bremner, T. and Rudin, A. *J. Polym. Sci., Polym. Phys. Edn* 1992, **30**, 1244
20 Lauritzen, J. I. and Hoffman, J. D. *J. Res. Natl Bur. Stand., Sect. A* 1960, **64**, 73
21 Abragam, A. 'Principles of Nuclear Magnetism', Oxford University Press, Oxford, 1961
22 Cohen-Addad, J. P. 'NMR and Fractal Properties of Polymeric Liquids and Gels', Pergamon Press, Oxford, 1991
23 Flory, P. J. 'Principles of Polymer Chemistry', Cornell University Press Ithaca, NY, 1953
24 Mark, J. E. 'Silicon-Based Polymer Science: A Comprehensive Resource', American Chemical Society, Washington, DC, 1990
25 Domard, M. PhD thesis, Université Joseph Fourier — Grenoble I, France, 1982
26 Wunderlich, B. and Cormier, C. M. *J. Chem. Phys.* 1966, **70**, 1844
27 Yim, A. and St Pierre, L. E. *J. Polym. Sci. (B)* 1970, **8**, 241
28 Cohen-Addad, J. P. *Polymer* 1992, **33**, 2762